Article

Journal of
Biomedical Nanotechnology
Vol. 11, 1947–1960, 2015
www.aspbs.com/jbn

Heparin and Vascular Endothelial Growth Factor Loaded Poly(L-lactide-co-caprolactone) Nanofiber Covered Stent-Graft for Aneurysm Treatment

Jing Wang[1,†], Qingzhu An[2,†], Dawei Li[1,3], Tong Wu[1], Weiming Chen[1], Binbin Sun[1], Hany El-Hamshary[4,5], Salem S. Al-Deyab[4], Wei Zhu[2,*], and Xiumei Mo[1,*]

[1] *State Key Lab for Modification of Chemical Fibers and Polymer Materials, Biomaterials and Tissue Engineering Laboratory, College of Chemistry and Chemical Engineering and Biotechnology, Donghua University, Shanghai 201620, P. R. China*
[2] *Department of Neurosurgery, Huashan Hospital of Fudan University, Shanghai, 200040, P. R. China*
[3] *Engineering Research Center of Technical Textiles, College of Textiles, Donghua University, Shanghai, 201620, P. R. China*
[4] *Department of Chemistry, College of Science, King Saud University, Riyadh 11451, Kindom of Saudi Arabia*
[5] *Department of Chemistry, Faculty of Science, Tanta University, Tanta 31527, Egypt*

Restenosis caused by thrombopoiesis is one of the biggest hinders of endovascular stent-graft used in small-diameter vessels. Rapid endothelialization of the lumen of stent is a promising approach to prevent thrombosis. In this study, we aimed at loading heparin, a potent anticoagulants, and vascular endothelial growth factor (VEGF) into the core of poly(L-lactide-co-caprolactone) nanofiber via emulsion electrospinning. The nanofiber was covered on the stent and applied in the treatment of vascular diseases such as aneurysm. The morphologies of the emulsion electrospun nanofibers and core–shell structure were observed by scanning electron microscope and laser scanning confocal microscope. The release profiles of heparin and VEGF, degradation rate of nanofiber mats and cell proliferation *in vitro* were investigated. It was found that the release of both heparin and VEGF from the nanofiber lasted for more than 30 days without serious initial burst release. The degradation rate of nanofiber mats containing heparin and VEGF was faster than that of pure PLCL nanofiber mats. Moreover, the released VEGF could promote the proliferation of Pig iliac endothelial cells (PIECs) cultured on the nanofiber mat, which was of great benefit to stent endothelialization. The results of digital subtraction angiography (DSA) follow-up indicated the aneurysm was obliterated by separating the aneurysm dome from the blood circulation and the parent artery kept long-term patency. Results of the study demonstrated that the heparin and VEGF loaded nanofiber could provide an approach to fabricate covered stent-graft with properties of anticoagulation and induction of rapid endothelialization.

KEYWORDS: *Heparin, VEGF, Nanofiber, Covered Stent-Graft.*

INTRODUCTION

Diseases of cerebrovascular system are the leading causes of death and disability in modern society, particularly in the developed countries.[1] Intracranial aneurysms are among the most common cerebrovascular diseases, with the annual incidence of 8–16 per 100,000 people,[2] and are increasingly regarded as the cause of devastating subarachnoid hemorrhage (SAH) which can lead to hemorrhagic stroke, brain damage and death.[3,4] An effective treatment of the cerebral aneurysm may maximally reduced the risk of aneurysm rupture. Last decade, covered stent has been proved to be an excellent option for arteriovenous fistulas, aneurysms, and aortic dissections.[5–9] Covered stent grafts have been used in peripheral vessels, thoracic aorta and abdominal aorta as an interventional treatment means for aneurysms therapy for many years, but there is still no ideal one dedicated to the treatment of cerebral aneurysm. Although the Willis covered stent which is specifically designed for use in the intracranial vasculature has exhibited great potential for the treatment

*Authors to whom correspondence should be addressed.
Emails: drzhuwei@fudan.edu.cn, xmm@dhu.edu.cn
†These two authors contributed equally to this work.
Received: 25 August 2014
Revised/Accepted: 5 November 2014

of aneurysms,[10–12] there have been several problems to be solved with this approach.[13,14] The implanted covered stent as a foreign body may cause platelet aggregation, leading to thrombosis and intimal hyperplasia, and the chronic irritation on the vascular wall can cause stent stenosis or restenosis, thus limiting the long-term efficacy of covered stent. Generally, a complete covered stent consists of a synthetic or natural material that either covers or is attached to a metallic stent to create a graft endoprosthesis. In addition to metallic stent, the coating material plays an important role in the incidence of stenosis after stent implantation.[15] The conventional artificial blood vessel materials such as expanded polytetrafluoroethylene (ePTFE),[16] Dracron[17] and polyurethane (PU)[18] which are working well in large-diameter vascular are not suitable for smaller intracranial arteries because of the aforementioned intimal hyperplasia, vascular stenosis resulting from thrombosis.[19,20] Therefore, a novel covered stent with anticoagulant matrix remains an urgent need to overcome these existing disadvantages for the intracranial aneurysms treatment.

Currently, the methods used to avoid thrombosis are more, among which rapid endothelialization, antithrombotic coatings, and anti-clotting drugs loading are common.[21–23] As a kind of natural polysaccharide compound, heparin not only has anti-inflammatory, anti-allergic effects, but also to some extent inhibits excessive proliferation of vascular smooth muscle cells (VSMCs)[24] and is currently the most widely used anti-clotting drugs. Heparin and other anticoagulants have been incorporated into biomaterials to inhibit intrinsic thrombogenicity.[21,25,26] Vascular endothelial growth factor (VEGF) is an essential signal protein produced by cells for stimulation of vasculogenesis and angiogenesis. VEGF can stimulate endothelialization with the ability of enhancing the adhesion and proliferation of vascular endothelial progenitor cells (VEPCs) and vascular endothelial cells (VECs),[27–32] and it could also inhibit excessive proliferation of VSMCs and attenuate neointimal hyperplasia.[33]

For rapid endothelialization to resist platelet adhesion and thrombosis, proliferation of VECs should be promoted on the lumen of the stent graft as soon as possible after transplantation.[34] For example, VEGF was immobilized to a gradient heparinized nanofiber graft to enhance adhesion and proliferation of human umbilical VECs on the lumen of blood vessel and prevent thrombosis.[35] However, it is worth noting the risks and negative effects of such drugs and growth factors at high concentration in the blood circulation, including serious heparin-induced thrombocytopaenia and bleeding,[36–38] and over-expressed VEGF resulting in intimal hyperplasia and the formation of giant lymphatic vessels and highly fenestrated capillary vessels similar to capillary vessels in tumors.[39–41] Furthermore, VEGF has a short half-life in body,[42] and it is easy to lose its biological activity during chemical and physical processing. Therefore, the controlled dosage of these drugs and proteins with protected bioactivity should be in the consideration for the medical therapy.[43–46]

Electrospun nanofiber is a stable and safe carrier for bioactive molecules, and many model drugs have been encapsulated into electrospun nanofiber for drug delivery application.[47–52] Coaxial and emulsion electrospinning have been developed as convenient and promising methods to incorporate bioactive substance into the core of electrospun nanofiber for biomedical applications.[53–57] In addition, electrospinning is reported to be an efficient process to fabricate scaffolds for tissue engineering applications as the electrospun nanofiber scaffolds can simulate the morphology and structure of natural extracellular matrix and provide a good microenvironment for cell adhesion and proliferation.[58–61] Till now, a lot of synthetic and natural polymers including polylactide (PLA),[62] poly(ε-caprolactone) (PCL),[63] poly(glycolic acid) (PGA),[64] collagen,[65] chitosan,[66] gelatin,[49] etc. have been electrospun into fibrous scaffold applied in tissue engineering. When the electrospun nanofiber mat is used as a stent coating layer of covered stent, better blood compatibility and minimal inflammatory responses *in vivo* will be obtained. Additionally, the heparin and VEGF loaded in the nanofiber scaffolds can be released in a sustained manner and play a role in lesion with minimal loss of biological activity.

For this purpose, heparin and VEGF were encapsulated into the biodegradable poly(l-lactide-co-caprolactone) (P(LLA-CL)) nanofiber scaffolds by emulsion electrospinning. Heparin has been incorporated into nanofibers in our previous study successfully.[67] In this research, the release behaviors of heparin and VEGF encapsulated in nanofibers were both investigated within the period of one month. The proliferation of VECs on the nanofiber scaffolds was also examined *in vitro*. Results indicated that the P(LLA-CL) nanofibers fabricated via emulsion electrospinning could preserve the bioactivity of heparin and VEGF, control the sustained release, and could be a good candidate for use in stent-graft.

MATERIALS AND METHODS

Materials

P(LLA-CL) (LA:CL = 50:50, Mw 300 kDa) was purchased from Gunze Limitted, Japan. Heparin (Hep, $\leq$150 U/mg), sorbitan monooleate (Span80) were purchased from Sigma-Aldrich Co, Ltd (St. Louis, USA). Dichloromethane and hexafluoroisopropanol (HFIP) were purchased from shanghai Fine-Chemicals Co, Ltd. (Shanghai, China). Recombinant human VEGF165 was supplied by Peprotech, USA. And enzyme-linked immunosorbent assay (ELISA) kit for VEGF was purchased from Neobioscience Technology Company (Shanghai, China). All culture media and reagents were purchased from the Gibco Life Technologies Co. (Carlsbad, California). Bare metal stents (stainless steel), stent

delivery balloon and guiding catheter were kindly provided by Shanghai MicroPort Co., Ltd. (Shanghai, China). All reagents for aneurysm creation were offered from HuaShan Hospital of FuDan University (Shanghai, China). All of the materials and reagents were used without further purification.

Fabrication of Nanofiber Scaffold

Preparation of Electrospinning Solution

Emulsion of P(LLA-CL) containing heparin and VEGF was prepared by 0.25 mL mixed aqueous solution with 20 μg VEGF and 37.5 mg heparin, and 0.05 mL span80 in 5 mL dichloromethane, and formed the uniform water-in-oil emulsion via magnetic stirring (300 rpm, 3 h). Subsequently, 0.4 g P(LLA-CL) was dissolved in emulsions and the mixture was stirred (300 rpm) overnight to obtain uniform electrospinning solution. Finally the solution was electrospun to obtain scaffold named as PLCL-Hep-VEGF.

Similarly, emulsion of P(LLA-CL) containing VEGF was prepared by the up-mentioned methods without adding heparin, and emulsion of P(LLA-CL) containing heparin was also made without adding VEGF. Followed with their separate processing by electrospinning, and the electrospun scaffolds were named as PLCL-VEGF, PLCL-Hep, respectively.

Pure P(LLA-CL) solution was prepared by dissolving 0.4 g P(LLA-CL) in 5mL HFIP. Then the solution was electrospun to obtain scaffold named as PLCL to serve as the control sample.

Fabrication of Fibrous Mats and Covered Stent-Graft

The electrospinning apparatus was equipped with a high voltage power supply (BGG DC high voltage generator), purchased from the BMEI Co., Ltd. (Beijing, China), and a digitally controlled and extremely accurate syringe pump (KDS 200), purchased from KD Scientific (Hollistton, MA). During electrospinning, a positive high voltage of 14 KV was applied at the tip of a syringe needle with the inner diameter of 0.7 mm. The electrospun nanofibers were collected on a piece of aluminum foil which was grounded. The distance between the needle and the collector was set as 10 cm. The flow rate of electrospun solution was maintained at 1.0 mL/h. The electrospinning was conducted under the ambient condition. All the fiber mats were dried in a vacuum oven overnight to remove the residual organic solvent and then stored at 4 °C for the further usage.

Similarly, the stent-graft covered with fibrous layer was also fabricated by electrospinning P(LLA-CL) containing heparin and VEGF emulsion. While the nanofibers were collected by a rotating rare metal stent (600 rpm, $\Phi =$ 2.7 mm, and $l = 13$ mm), which was fixed by the inner smaller metal rods.

Characterization of Nanofiber Scaffold

Scanning Electron Microscopy

The morphology of the fabricated nanofibers was examined by Digital Vacuum Scanning Electron Microscope (JSM-5600LV, Japan Electron Optical Laboratory) at the accelerating voltage of 15 KV. Prior to scanning electron microscopy (SEM) examination, the samples were sputter coated with gold to avoid charge accumulation.

Laser Scanning Confocal Microscopy

Fluorescein isothiocyanate conjugated BSA (FITC-BSA) was used as the stabilizer to study the distribution of VEGF in the nanofibers, by observing the FITC-BSA distribution in the fabricated nanofibers by laser scanning confocal microscopy (LSCM) (Zeiss LSM 700, Germany).

Fourier Transform Infrared Spectroscopy

In order to determine the encapsulation of heparin in nanofiber, the chemical components of samples were tested by Fourier Transform infrared spectroscopy (FTIR) (Thermo Electro AVATAR 380, USA).

X-ray Diffraction

The samples were also tested using an X-ray diffraction instrument (D/MAX-2550PC, Rigaku, Japan). A voltage of 40 kV and a current of 300 mA using a CuKα radiation ($\lambda = 1.5418$).

Mechanical Properties

Mechanical properties were obtained by applying tensile loads to specimens of different nanofiber scaffolds. For mechanical test, five specimens (30 mm $\times$ 10 mm) of each sample were prepared according to the method described by Huang et al.[68] The tensile testing was performed using a universal materials testing machine (H5K-S, Hounsfield, England) at ambient temperature and a relative humidity of 65%. A cross-head speed of 10 mm min^{-1} was used for all specimens tested. Before testing, all samples were soaked in PBS for 2 h. Ultimate tensile stress, elastic modulus, and strain at break was determined. As control, the dry samples had also carried on the tensile test under the same condition.

Entrapment Efficiency of Heparin and VEGF

The entrapment efficiency of heparin and VEGF in the PLCL-Hep-VEGF nanofibers were determined according to the method described by Yan et al.[69] In brief, a known amount of fibers (around 20 mg) containing heparin and VEGF was dissolved in 4 mL dichloromethane/PBS solution. The mixture was vortexed for 1 min followed by centrifugation at 4000 rpm for 5 min. This would cause phase transfer with P(LLA-CL) moved to the organic phase while heparin and VEGF moved to the aqueous phase. Then the aqueous supernatant was removed for

testing. The content of heparin was determined by toluidine blue method and that of VEGF was determined by the VEGF ELISA kit. All samples were tested in triplicate. The entrapment efficiency was calculated as the ratio of heparin (VEGF) loaded, estimated from the supernatant, to the total heparin (VEGF) added to the electrospinning solution actually.

In Vitro Release Profile of Heparin and VEGF

For evaluating the release behavior of heparin and VEGF from the nanofibers, composite nanofiber scaffolds loaded with both heparin and VEGF as well as two control samples (only loaded with heparin or VEGF), each weighing about 50 mg, were immersed in a 15 mL centrifuge tube with 5 mL phosphate-buffered saline (PBS, pH 7.4). The nanofiber scaffolds were incubated in a continuous horizontal shaker which was maintained at 37 °C and 100 cycles/min. At predetermined time points, the release buffer was removed from the tube for analysis and an equal volume of fresh PBS was added for following incubation. The quantity of heparin and VEGF in the release buffer was determined by toluidine blue and human VEGF kit, respectively. The results were expressed by cumulative release as a function of release time: Cumulative amount of release $(\%) = M_t/(M_0 \times X) \times 100$, where M_t is the weight of heparin (VEGF) released at time t and M_0 is the total amount of heparin (VEGF) in the fibers theoretically. X is the entrapment efficiency measured in the last step. Triplicate specimens were analyzed in each sample.

In Vitro Degradation of Nanofiber Scaffold

In order to evaluate the effect of emulsifier and loaded drugs on the degradation performance of nanofiber scaffold, PLCL and PLCL-Hep-VEGF nanofiber mats were preweighted (50 mg each) and added to 10 mL of PBS which contain 0.02% sodium azide as a bacteriostatic agent (pH 7.5). All the samples were placed in concussion incubator at 37 °C. At predetermined time points, a group of each was retrieved, rinsed with distilled water to remove residual buffer salts, and freeze-dried using freeze dryer and preserved in a vacuum oven. Then a series of analyses (including changes of morphology, mass loss and pH changes of PBS solutions) were conducted to the nanofiber mats after the degradation. All samples were assayed in triplicate.

Cell Seeding

Pig iliac endothelial cells (PIECs) (purchased from Institute of Biochemistry and Cell Biology of the Chinese Academy of Sciences, Shanghai, China) were used to evaluate the bioactivity of VEGF released from nanofiber mats. PIECs were cultured in DMEM medium with 10 wt% fetal bovine serum and 1 wt% antibiotic-antimycotic (100 units mL^{-1} Penicillin and 100 units mL^{-1} streptomycin) in a humidified incubator with 5% CO_2 and 37 °C. The medium was refreshed every three days. The medical-grade cover-slips (14 mm in diameter) were placed on the aluminum foil to collect the nanofibers during electrospinning. The slips were removed from the aluminum foil and fixed on 24-well plates by stainless steel rings. Then all samples were sterilized with 75 vol% alcohol steam. After sterilization, the samples were washed with PBS for three times and 100 μl of medium was added into each well. Then the 24-well plates were put into the incubator and incubated for 1 hour. PIECs were seeded onto nanofiber mats at a cell density of 1×10^4 cells/well.

Cell Proliferation

The cell proliferation on different nanofiber mats was quantified by the standard 3-[4, 5-dimethyl-2-thiazolyl]-2, 5-diphenyl-2H-tetrazolium bromide (MTT) assay ($n = 3$). After culturing for a period of 1, 3, 5, 7 days, the medium was removed and the samples were rinsed with PBS to remove the unattached cells. Then 40 μL MTT reagent and 360 μL serum-free medium were added into each well and incubated for 4 h at 37 °C. Thereafter, the culture medium was extracted and 400 μL dimethylsulfoxide (DMSO) was added and incubated in a continuous horizontal shaker for 20 min. When the purple crystal was sufficiently dissolved, solution was pipetted into a 96-well plate and measured at 492 nm by a spectrophotometric plate reader (Multiskan MK3, Thermo, USA).

Cell Morphology

For cell morphology analysis, SEM was used to observe PIECs morphologies on nanofiber mats. PIECs were seeded onto nanofiber mats ($n = 2$) at a density of 10^4 cells/well for 3 days. After 3 days, the culture media were extracted and the cells loaded fiber mats were rinsed twice with PBS and fixed with 4% paraformaldehyde for 2 h at 4 °C. Following twice rinses with distilled water, the fixed samples were dehydrated through a serious of graded ethanol solution (30, 50, 70, 80, 90, 95, and 100%) and then freeze-dried. Finally, the dry samples were sputter-coated with gold and observed under the SEM at a voltage of 10 kV.

The laser confocal scanning microscopy (LCSM) was used to visualize cells spreading and morphology on the nanofiber mats. The cell-seeded scaffolds were fixed by 4% paraformaldehyde for 30 min, followed by rinsing with PBS for three times. Then the cells were permeabilized with 0.1% Triton X-100 (Sigma, USA) for 5 min. The actin filaments of PIECs were stained into red by rhodamine-conjugated phalloidin (Invitrogen, USA) and the cell nucleus were stained into blue by 4′, 6-diamidino-2-phenylindole (DAPI) (Invitrogen, USA). The mounted samples were observed by LSCM (Zeiss LSM 700, Germany).

In Vivo Examination

In order to evaluate the safety and effectiveness of the fabricated covered stent-graft for the treatment of aneurysm, the covered stent-graft was implanted into the parent artery of New Zealand white rabbit. Saccular aneurysms were created in New Zealand white rabbits (2–3 kg) according to the method shown in the Refs. [67, 70]. After successful aneurysm creation was confirmed with digital subtraction angiography (DSA), the covered stent-graft was implanted in the innominate-to-subclavian artery with the intent of maintaining equal lengths on either side of the aneurysm ostium. Details of the migration process have been described in our previous study.[67] DSA was used to evaluate aneurysm blood flow at different time points (1, 3 months) after stenting. The covered stent-grafts were removed from the body after stenting for 3 months and the endothelialization of parent artery was observed by SEM. The stent–graft covered with expanded polytetrafluoroethylene (ePTFE) was chosen as the control group and was also implanted into the parent artery of New Zealand white rabbits with aneurysm models. Three parallel tests were used for each experimental group and control group. All animal procedures were approved by the HuaShan Hospital of FuDan University (Shanghai, China).

Statistical Analysis

All results are expressed as the means ± standard deviation (SD). Statistical analyses were performed with one-way ANOVA analysis, followed by Tukey's test with Origin Pro 8.0 (Origin Lab, USA). $p < 0.05$ was considered to be significant difference.

RESULTS

Characterization of Nanofiber Scaffold

Scanning Electro Microscopy

The nanofiber scaffold based on P(LLA-CL) with heparin and VEGF encapsulated was fabricated by emulsion electrospinning. As a control, pure P(LLA-CL) nanofibers were fabricated by general electrospinning. Figure 1 shows the SEM micrographs of the obtained nanofiber scaffolds. The nanofiber in the scaffolds was continuous, smooth, and beadless. However, some conglutination occurred to the electrospun nanofiber loaded with heparin and VEGF at the junction zones. This maybe resulted from that the fibers were not completely dried during the electrospinning process. Water incorporated into the emulsion drops was difficult to evaporate when the surfactant was added. The diameter of PLCL-Hep-VEGF nanofibers was much thinner than that of pure PLCL nanofibers because of the addition of charged solute.

Fourier Transform Infrared Spectroscopy

According to the FTIR spectrum (Fig. 2(a)), the typical absorption peak of heparin (1640 cm^{-1} (amide I) caused by –C═O stretching of $–CONH_2$ group) appeared in PLCL-Hep and PLCL-Hep-VEGF nanofibers. This result demonstrated that heparin had been incorporated into the fibers.

Laser Scanning Confocal Microscopy

The distribution of VEGF inside the nanofibers was observed by LSCM. BSA is usually used as the carrier protein to protect the bioactivity of growth factors. So the FITC-BSA was used to confirm the distribution of VEGF in the core of nanofibers. Figure 2(b) is the fluorescein image of the nanofibers containing VEGF and FITC-BSA. The result observed by LSCM indicates the distribution of FITC-BSA inside the nanofibers. The emitted green fluorescent light suggested the presence of proteins in the nanofibers.

X-ray Diffraction

Figure 3 presents the XRD patterns of different composite nanofiber (a) and heparin powder (b). It was shown that heparin was crystalline, with many characteristic peaks. The heparin was detected in all fibers containing heparin. In addition, the heparin existed in the nanofibers kept its original crystal structure. So there was no chemical reaction between heparin and P(LLA-CL) polymer.

Mechanical Properties

Tensile mechanical tests were conducted on PLCL and PLCL-Hep-VEGF scaffolds to determine the effect of emulsifier and drugs on the mechanical property of scaffold. Figure 4 shows stress–strain curves of scaffolds under tensile loading. Compared with the mechanical properties

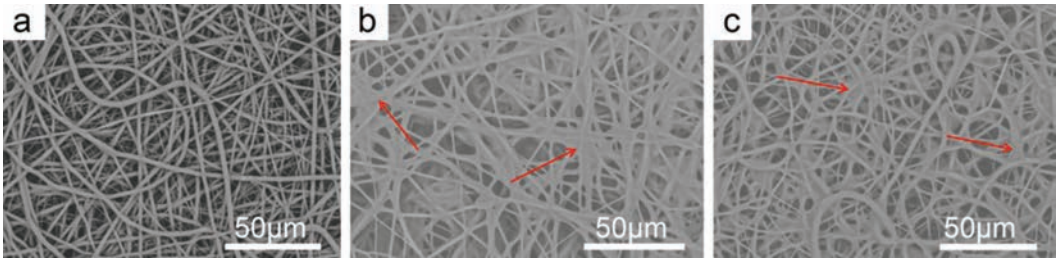

Figure 1. SEM images of electrospun nanofibers. (a) PLCL, (b) PLCL-Hep, and (c) PLCL-Hep-VEGF. Red arrows denote the conglutination occurred between fibers.

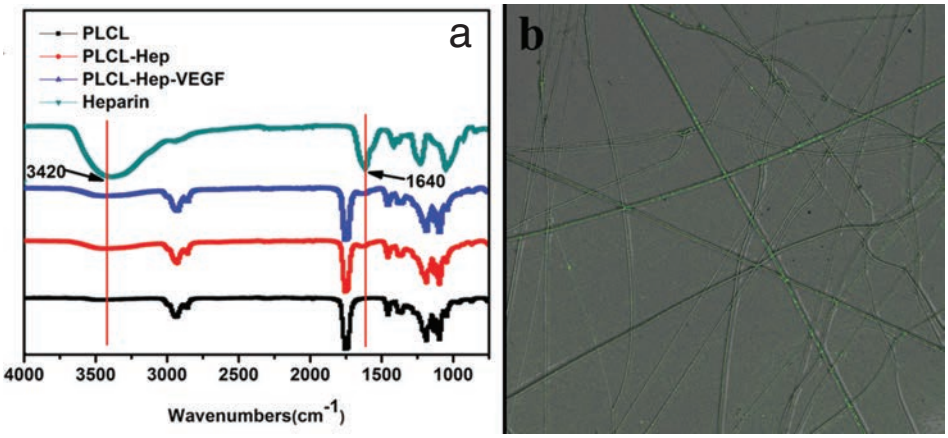

Figure 2. **(a) The FTIR spectra of PLCL, PLCL-Hep, PLCL-Hep-VEGF and Heparin. (b) Laser scanning confocal microscopic images of core–shell nanofibers with FITC-BSA.**

under dry state, the tensile strength of both scaffolds treated with PBS decreased, while the elongation changed little. Whether it was dry or wet, both the tensile strength and elongation of PLCL nanofiber scaffold was a bit higher than that of PLCL-Hep-VEGF nanofiber scaffold.

In Vitro Release Profile of Heparin and VEGF

The entrapment efficiency of heparin in PLCL-Hep-VEGF and PLCL-Hep nanofibers was $62.8 \pm 4.5\%$ and $63.5 \pm 5.8\%$, respectively. The encapsulation efficiency of VEGF in PLCL-Hep-VEGF and PLCL-VEGF were $65.8 \pm 4.3\%$ and $63.2 \pm 4.9\%$, respectively. The release profile of heparin from the composite nanofibers for one month is showed in Figure 5(a). It was found that release behavior of heparin from PLCL-Hep-VEGF is similar to that from PLCL-Hep. This was due to amount of VEGF was much less than that of heparin. So the existence of VEGF did not affect the release behavior of heparin from the nanofibers. A burst release of $12.0 \pm 1.9\%$ was detected during the initial 24 h, followed with a constant fast release for 150 h, and then a slow release pattern. Heparin located on the fiber surface resulted in the initial bust release. Then the heparin near the surface released faster in the form of diffusion release. Finally, the heparin incorporated into the innermost of nanofiber released slower through the nanofiber matrices. Figure 5(b) shows the release profile of VEGF from PLCL-Hep-VEGF and PLCL-VEGF nanofiber scaffolds in the same condition. The entire release process can be divided into two stages. The release quantity for PLCL-Hep-VEGF and PLCL-VEGF scaffolds during the first release stage was about 6.5 and 18.5%, respectively. After the second release stage, the cumulative release quantity for PLCL-Hep-VEGF and PLCL-VEGF scaffolds was about 23.4 and 40.1%, respectively. The release profile of the two scaffolds varied greatly.

In Vitro Degradation of Nanofiber Scaffold

The mass loss of PLCL and PLCL-Hep-VEGF nanofiber mats is summarized in Figure 6(a). There was more mass loss of PLCL-Hep-VEGF than that of PLCL nanofiber mats after the same incubation time. The pH changes of PBS buffered solution with nanofiber mats for different degradation time are shown in Figure 6(b). The pH

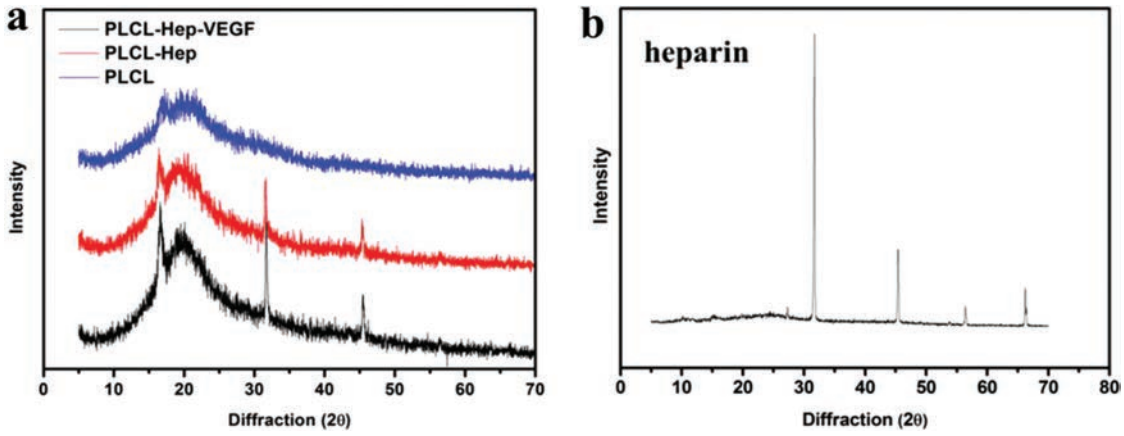

Figure 3. **The XRD patterns of different composite nanofiber (a) and heparin powder (b).**

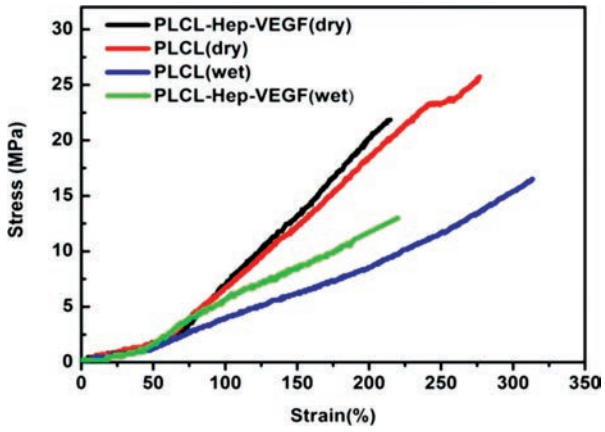

Figure 4. **The stress–strain curves of nanofiber mats.**

value of PBS solution was declining with the increase of incubation time. The pH of degradation medium with PLCL-Hep-VEGF nanofiber mats was lower than that of PLCL. SEM images of electrospun PLCL and PLCL-Hep-VGEF nanofiber mats after degradation for 1, 2, 3 and 4 months are shown in Figure 6(c). After degradation for 1 month, PLCL nanofiber mat had no obvious change but slight swelling. However, the fiber breakages of PLCL-Hep-VEGF nanofiber mat were observed due to the release of heparin and VEGF. After degradation for 3 months, fiber morphology was not observed on the surface of PLCL-Hep-VEGF nanofiber mat, while the fiber structure still could be observed on the surface of PLCL nanofiber mat. The results indicated that the additions of emulsifier, heparin and VEGF promoted the degradation of nanofiber mat.

Cell Proliferation

A MTT assay was utilized to evaluate the proliferation of cells. PIECs were cultured on the electrospun nanofiber scaffolds, including PLCL, PLCL-Hep, PLCL-Hep-VEGF and cover slips to exam the influence of the released VEGF on the cells proliferation. PLCL nanofiber scaffold with the addition of an equivalent amount of free VEGF were also determined (PLCL/VEGF) as the control group. The proliferation of PIECs obtained by MTT assay is showed in Figure 7. It was observed that the cells proliferated faster on all nanofiber scaffolds than that on cover slips. It also indicated that either the direct addition or the encapsulation of VEGF improves the PIECs proliferation on nanofiber scaffolds. With respect to them, the cells on PLCL nanofiber scaffold with the addition of free VEGF (PLCL/VEGF) showed faster growth than that on PLCL-Hep-VEGF nanofiber scaffold on day 1. However, the cells growth on PLCL-Hep-VEGF nanofiber scaffold is obviously higher than that of PLCL nanofiber scaffold with free VEGF addition on day 3, 5 and 7. Moreover, the difference became more significant with the increase of culture time. The loading of heparin with this amount showed no significant influence on PIECs proliferation. Statistically, the VEGF loaded in the nanofiber released in a sustainable manner could stimulate the cells growth continuously.

Cell Morphology

Figure 8 shows the SEM micrographs of PIECs cultured on all scaffolds for 3 days. It could be clearly seen that the cells attached and stretched on the scaffolds and cover slips. In addition, the electrospun PLCL-Hep-VEGF nanofiber scaffold provided a more excellent microenvironment than PLCL and PLCL-Hep nanofiber scaffolds for PIECs attachment and proliferation because of the existence of VEGF. The cells cultured on PLCL-Hep-VEGF nanofiber scaffold showed better interactions in comparison with PLCL and PLCL-Hep nanofiber scaffolds. A very limited number of cells were attached on PLCL nanofiber scaffold, whereas the number of cells cultured on PLCL-Hep-VEGF nanofiber scaffold reached an estimated confluence of about 80%. As shown in Figure 8, the confocal laser micrographs of PIECs on various scaffolds on day 4 showed more exquisite spread on PLCL-Hep-VEGF than on PLCL and PLCL-Hep. All of these results indicate that the VEGF released from the nanofiber scaffold with high biological activity stimulates the growth of PIECs.

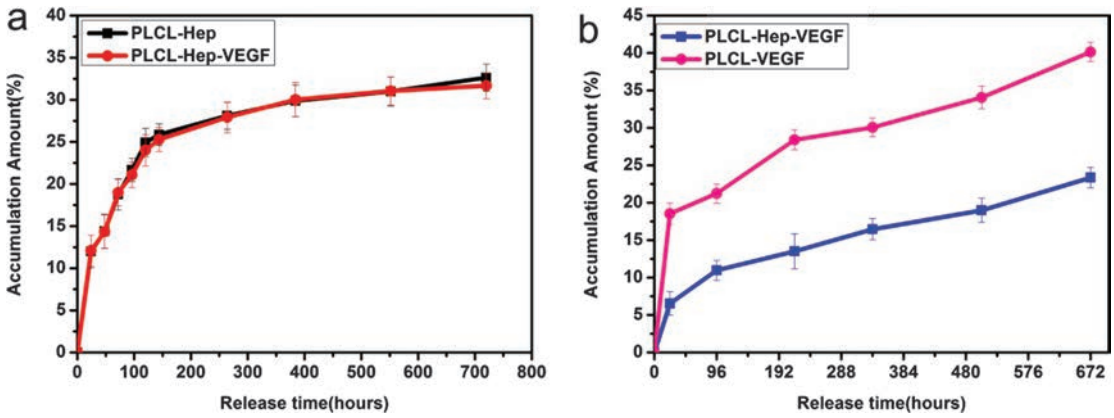

Figure 5. **Release profiles of heparin (a) and VEGF (b) from emulsion electrospun nanofibers.**

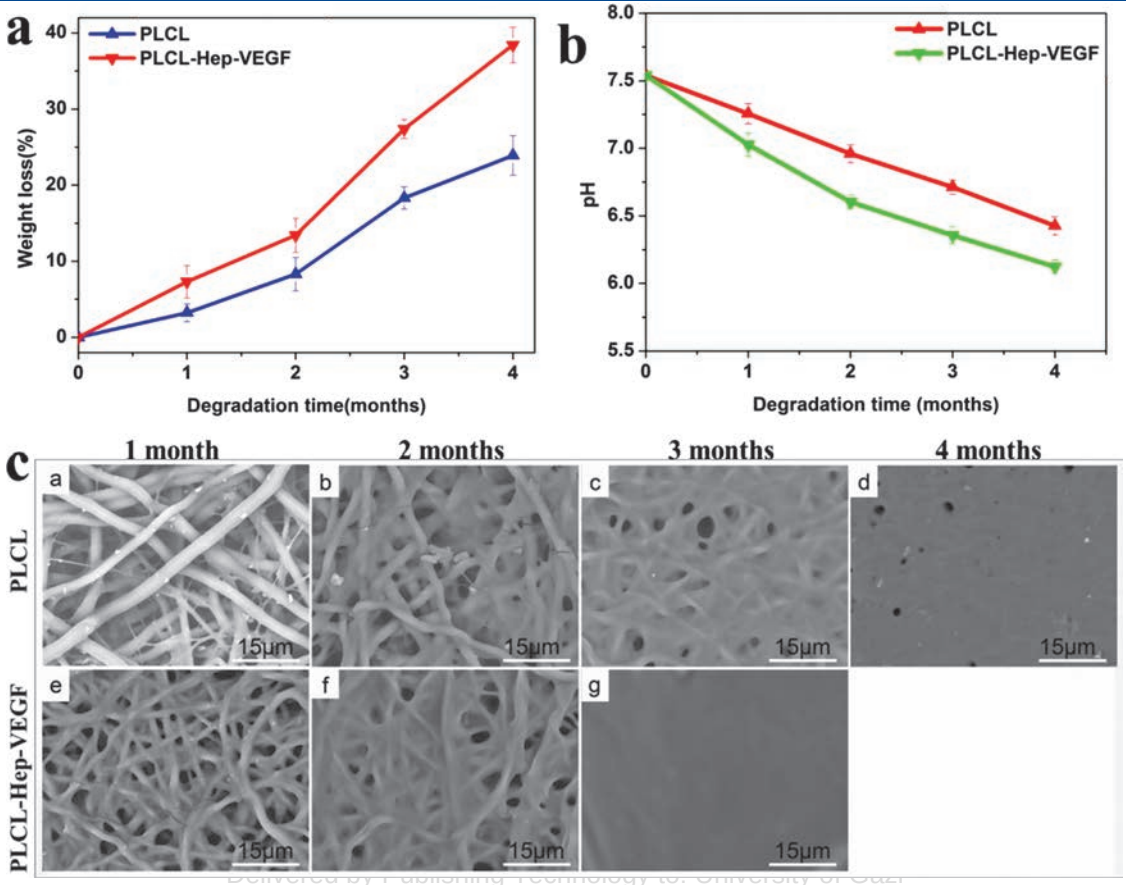

Figure 6. ***In vitro*** **degradation profiles of electrospun nanofiber mats. (a) Weight loss of nanofiber mats, (b) pH changes of PBS after incubated at 37 °C, (c) morphologies of PLCL and PLCL-Hep-VEGF nanofiber mats after incubated in PBS for 1, 2, 3, 4 months.**

Fabrication of Covered Stent-Graft

The covered stent-graft was prepared using a conventional electrospinning setup (Fig. 9(b)). An earthed rotating bare metal stent (Fig. 9(c)) was set on a rotating metal stick (Fig. 9(a)) to collect nanofibers directly, and the formed thickness of the electrospun layer was in the range of 120–150 μm. Figure 9(d) shows the fabricated covered stent-graft covered with nanofibers containing heparin and VEGF.

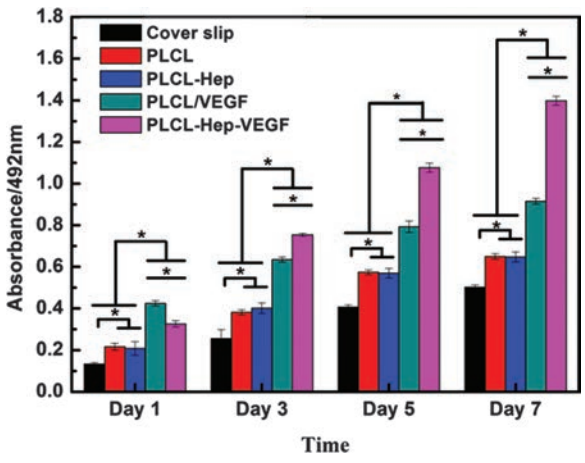

Figure 7. **The proliferation of PIEC on cover slip and different electrospun nanofiber mats. *Indicates significant difference of $p < 0.05$.**

In Vivo Examination

Figure 10(a) shows that the rabbit aneurysm model simulated the morphology and hemodynamics of human cerebral aneurysm was successfully created in all cases without morbidity or mortality. The angiogram before stenting (Fig. 10(b)) revealed direct flow into the aneurysm of right common carotid artery stump. After stenting, the aneurysm was obliterated immediately (Fig. 10(c)). All rabbits were healthy without any observable neurological deficit over the course of experiments. No difference was found in diet intake and behavior before and after surgery. The treatment effect of aneurysm models and patency of parent artery in the short term (2 weeks) after stenting has been observed in our previous research.[67] Angiogram at 1 month follow-up (Fig. 11(a)) shows that the aneurysm was still invisible in all three cases of experimental group. But recurrence of the aneurysm occurred in one case of control group (Fig. 11(d)). After 3 months of stenting, aneurysms of all three cases of experimental group were

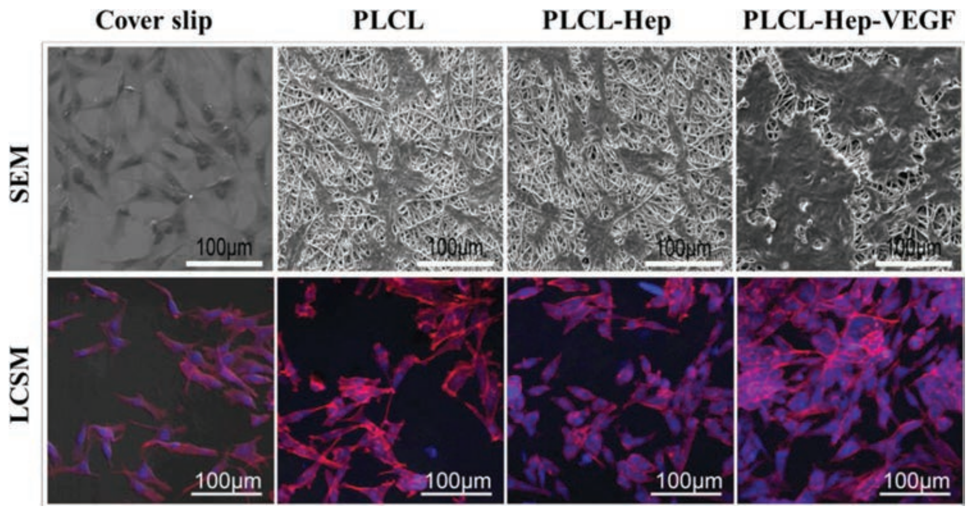

Figure 8. SEM micrographs and LCSM micrographs for PIECs cultured on cover slip and different electrospun nanofiber mats on day 3.

still not relapse and no stenosis or intima hyperplasia in parent artery (Fig. 11(b)). However, occlusion of the parent arteries could be seen in one case of control group (Fig. 11(e)). This was due to the thrombosis resulted of the platelet aggregation and intimal hyperplasia in control group. The covered stent-graft containing heparin and VEGF used in the experimental group could prevent the aggregation of platelet effectively. After angiography, all animal models were put to death, the parent artery with covered stent graft was removed from body and fixed with glutaraldehyde after slitting. Finally, the surface of covered stent-graft was observed using SEM. The results of SEM showed that there was a more complete endodermis in covered stent-graft of experimental group than that of control group. The surface of bare metal stent covered with nanofibers containing heparin and VEGF was covered by endodermis completely (Fig. 11(c)). On the contrary, exposed metal stent can still be seen in covered stent-graft with ePTFE in control group (Fig. 11(f)). Therefore, the results indicated that the VEGF and heparin loaded in the nanofibers can prevent vascular thrombosis and neointimal hyperplasia after stenting.

DISCUSSION

The implanted covered stent-graft do not mimic the anticoagulant properties of native blood vessels and may cause complications that involve thrombosis and restenosis, thus limiting the long-term efficacy of it in intracranial aneurysm treatment. The conventional artificial materials used in covered stent-graft such as expanded polytetrafluoroethylene (ePTFE), Dacron and polyurethane (PU) which working well in large-diameter vascular are not suitable for smaller intracranial arteries because of poor long-term

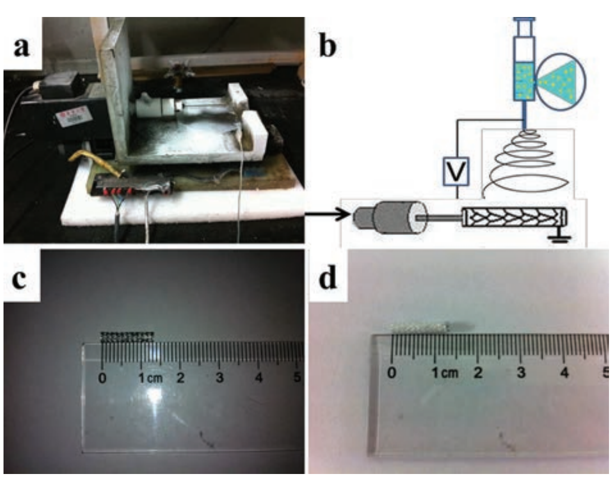

Figure 9. The scheme of fabrication of covered stent-graft (a), (b), digital images of bare metal stent (c) and covered stent-graft (d).

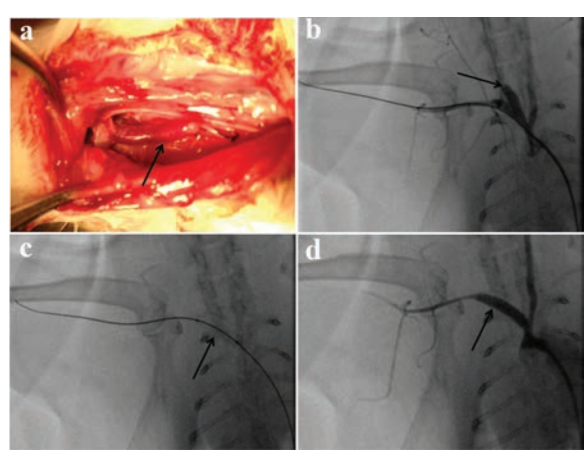

Figure 10. (a) The rabbit saccular aneurysm model after surgery. (b) The angiogram of aneurysm model before stenting. (c) The angiogram of the location of covered stent-graft in parent artery after stenting. (d) The aneurysm was obliterated immediately after stenting.

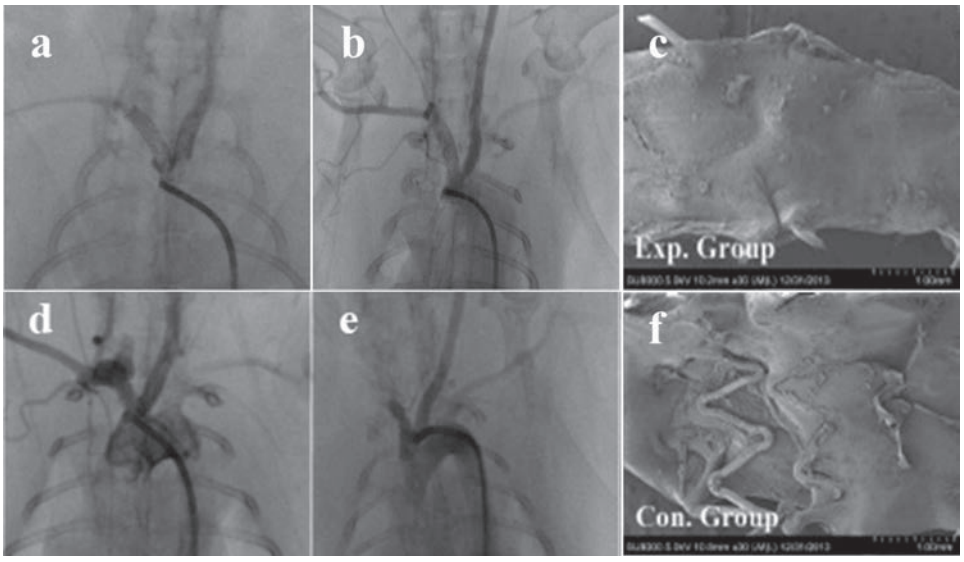

Figure 11. **The angiograms of experimental group after stenting for 1 month (a) and 3 months (b), The angiograms of control group after stenting for 1 month (d) and 3 months (e), The SEM images of the endovascular surface of experimental group (c) and control group (f) after stenting for 3 months.**

patency. The quest for the ideal covered stent-graft has generated a great amount of research. Heparin and other anticoagulants have been incorporated into stent graft via various strategies such as physisorption, electrostatic deposition and covalent bonding.[21, 23, 71–73] For example, heparin has been immobilized to the surface of cross-linked collagen to improve blood compatibility.[71]

Rapid endothelialization of the lumen of stent is a promising approach to prevent thrombosis. For rapid endothelialization to resist platelet adhesion and thrombosis, proliferation of VECs should be promoted on the surface of stent graft after stenting.[34] VEGF can stimulate endothelialization by enhancing adhesion and proliferation of VECs. Although some results have been achieved in anticoagulant and endothelialization through heparin-modification or immobilization of VEGF, there are still many deficiencies.[35] The release of heparin or VEGF from the scaffold cannot be controlled. Coaxial and emulsion electrospinning have been developed to incorporate bioactive molecules into nanofibers for biomedical applications.[56, 74]

In this study, we fabricated nanofibers loading heparin and VEGF via emulsion electrospinning. We also fabricated a novel covered stent-graft with nanofiber mat containing heparin and VEGF. P(LLA-CL) was chosen for the fabrication of nanofiber mat, as its excellent mechanical properties, biocompatibility and biodegrability have been shown in previous studies.[75, 76] The fabricated nanofibers were characterized in terms of their surface morphology, mechanical properties. The cell-scaffold interactions will be affected by the surface properties of scaffold. The SEM images showed that the nanofiber was continuous, smooth, and beadles. The hydrophilicity of nanofiber mat can be improved with the addition of emulsifier and loaded drugs[77] and this could be more beneficial for cell adhesion and proliferation.[78] The results of mechanics property test showed that the tensile strength of both scaffolds decreased after being treated with PBS for 2 h. Because the water penetrated into the matrix and led to hydrolytic cleavage of ester bonds and make the fibers easier to break. Moreover, the results demonstrated that both the tensile strength and elongation of PLCL nanofiber scaffold was a bit higher than that of PLCL-Hep-VEGF nanofiber scaffold. This could be contribute to the difference of mean diameters of fibers. The mean diameter of PLCL fibers (1990±392 nm) is larger than that of PLCL-Hep-VEGF fibers (1120± 186 nm). Besides, the heparin and VEGF loaded in fibers contributed much less to the mechanical performance of fiber mat. Our previous study found that the pure PLCL fiber coating layer could keep its morphology and structure and would not rupture with the expansion of covered stent-graft (from 2.7 mm to 4.0 mm) when its stress and strain were respectively 11.787±1.45 MPa and 182.347± 11.90%.[67] So the mechanical properties of PLCL-Hep-VEGF nanofiber mat can fully satisfy the requirement of covered stent-graft. Furthermore, the encapsulation of heparin in the fiber was confirmed by FTIR, and the distribution of VEGF mixed with FITC-BSA was observed inside the nanofibers by LSCM. In addition, the XRD patterns of different composite nanofiber and heparin powder proved that there was no chemical reaction between heparin and P(LLA-CL) polymer.

Our results showed a quick release of VEGF during the initial release period and became a sustained manner in the later period (Fig. 5). While the initial release amount from the fibers made by emulsion electrospinning is lower than the reported release amount of VEGF from the blended fibers.[54, 56] This is because the proteins (VEGF) are mainly

distributed on or adjacent to the surfaces of the fibers and most of them will get instantly release when it is immerged in PBS solution.[36] On the contrary, the proteins are wrapped inside the fibers fabricated by emulsion electrospinning, leading to the loaded proteins could be released in a sustained and controlled manner. In addition, the release results also indicated that heparin release did not show any difference between fibers with and without VEGF loading, while the VEGF release was significantly affected by the heparin loading. This might due to VEGF165 is a heparin-binding growth factor, thus, the release of heparin and VEGF in the combined component may both be affected by their binding, while huge amount of heparin compared to VEGF (the weight ratio between heparin and VEGF is 7.5×10^3) loaded in the fibers, could make the binding effect negligible for evaluating the total (VEGF binding and not binding) heparin release from the fibers, but this influence was significant for VEGF release results. Previous studies have also shown that the release of growth factors can be delayed when the heparin is introduced to the controlled release system.[38, 79]

A biodegradable polymer-based tissue engineering scaffold must be able to maintain suitable degradation rates. To evaluate the effect of emulsifier and protein incorporation on the degradation profile of electrospun nanofiber scaffold, the mass loss and morphology changes were detected for matrix residues of PLCL and PLCL-Hep-VEGF nanofiber mats.

The pH value change of degradation medium was also determined. In degradation process, the weight loss was caused by the diffusion and dissolve of soluble oligomeric compounds from the surface of polymer generated by the hydrolysis scission of polymer chains in the degradation medium. The release of heparin and VEGF will form cavities and holes on fibers and this will allow a thrust flow of PBS to the deeper layers of fibers.[80] So this will result of fast degradation of the matrix materials. In addition, the hydrophilcity of PLCL-Hep-VEGF was improved compared with PLCL nanofiber mats. This may also lead to faster degradation of the matrix materials. The decrease of pH in degradation medium was caused by soluble oligomers with carboxyl (—COOH) groups diffused and dissolved in the degradation medium from the nanofiber mats.[81]

Otherwise, the in addition, heparin is strongly acidic. So the pH of degradation medium with PLCL-Hep-VEGF nanofiber mats was lower than that of PLCL after degradation of the same time. The polymer chains become mobilized when glass transition temperature (T_g) of polymer is near or below the degradation temperature (37 °C) so that the fibers tend to melt together to reduce the surface tension.[42] Therefore, electrospun nanofibers based on P(LLA-CL) melted together along with the degradation because of the good elasticity and a lower T_g (−13.62 °C). On the whole, the release of heparin and VEGF from PLCL-Hep-VEGF nanofiber mat led to much pores in the fibers and this may result in faster distribution of water into the fiber matrix and faster hydrolysis of polymer.

It is important to evaluate the biocompatibility of the scaffold used for tissue engineering application. Many studies have shown that VEGF can stimulate endothelialization with the ability of promoting ECs proliferation.[27, 42, 43] A MTT assay was utilized to evaluate the proliferation of cells. The OD values on day 1, 3, 5, and 7 proved that the cells proliferated faster on all nanofiber scaffolds than that on cover slips. Either the direct addition or the encapsulation of VEGF improved the PIECs proliferation on nanofiber scaffolds. Because compared with PLCL-Hep-VEGF, the concentration of VEGF in the well containing PLCL/VEGF was larger on day 1. But there was more VEGF released from PLCL-Hep-VEGF scaffold with the increase of culture time, so the cells seeded on PLCL-Hep-VEGF proliferated faster than that on PLCL/VEGF after three days of culturing. Overall, the VEGF released from fibers maintained its biological activity and played a significant role in the proliferation of PIECs. In addition to cell proliferation, cell morphology is also an important aspect of biocompatibility evaluation of scaffold.[82] PIECs cultured on the nanofiber scaffold exhibited flatten morphology (Fig. 8) which was reported to be the special cell morphology of endothelial cells located inside blood vessels.[83] Compared with the cells on cover slips, cells on nanofiber scaffold presented the trend of formation of endodermis, especially the cells on PLCL-Hep-VEGF scaffold. PIECs developed a confluent monolayer on the surface of PLCL-Hep-VEGF scaffold. This suggested that VEGF released from the scaffold could effectively promote the endothelial.

The P(LLA-CL) emulsion containing heparin and VEGF was prepared according to the method mentioned above. Then the covered stent-graft was fabricated by emulsion electrospinning. In order to evaluate the safety and effectiveness of the fabricated covered stent-graft for the treatment of aneurysm, the covered stent-graft was transplanted into the parent artery of New Zealand white rabbit. After stenting, the aneurysm was obliterated immediately (Fig. 10(c)). There has been no recurrence of aneurysms of animal models which had implanted covered stent-graft containing heparin and VEGF and the parent artery remained unblocked after stenting for 3 months. On the other hand, the aneurysm appeared again in one case of animal models which had covered stent-graft with ePTFE in control group after stenting for 1 month. The possible reason was that the elastic properties of ePTFE is not good and a small rupture happened with the expansion of covered stent-graft. As the blood flow scouring, crevasse increased gradually and led to a recurrence of the aneurysm. After stenting for 3 months, occlusion of the parent arteries could be seen in one case of control group. Because anticoagulant property of ePTFE was poor and

did not form a complete endodermis. The covered stent-graft containing heparin and VEGF used in the experimental group could prevent the aggregation of platelet and the formation of endodermis effectively. The result indicated the aneurysm can be obliterated by separated the aneurysm dome from the blood circulation and the parent artery keep long-term patency after implanted covered stent-graft containing heparin and VEGF.

These promising results suggested that nanofibers loading heparin and VEGF fabricated by emulsion electrospinning could well control the release of heparin and VEGF and keep the biological activity of them. Rapid re-endothelialization onto the surface of implanted covered stent-graft may be an effective strategy to improve the treatment effect of aneurysm and prevent the parent artery stenosis. Our study demonstrated that the nanofiber mat containing heparin and VEGF can be used as the coating layer of covered stent-graft which can effectively cure the aneurysm and keep long-term patency of parent artery.

CONCLUSION

In this paper, nanofibers incorporating heparin and VEGF were fabricated by emulsion electrospinning. *In vitro* release study demonstrated that the PLCL-Hep-VEGF nanofibers could deliver heparin and VEGF in a sustained manner without serious initial bust. The cells culture results confirmed good biocompatibility of the electrospun scaffolds. The VEGF released from the nanofibers enhanced PIECs proliferation and spread on the scaffolds. The bioactivity of VEGF can be well protected by the nanofiber. The result of DSA follow-up indicated the aneurysm can be obliterated by separated the aneurysm dome from the blood circulation and the parent artery keep long-term patency. These findings showed the potential of heparin and VEGF loaded nanofibers fabricated by emulsion electrospinning for covered stent-graft application in aneurysm treatment.

Acknowledgments: This research was supported by the National Natural Science Foundation of China (No. 31470941 and 31271035), Science and Technology Commission of Shanghai Municipality (11 nm 0504100, 11 nm 0506200 and 124119a6402), Ph.D. Programs Foundation of Ministry of Education of China (20130075110005), Shanghai Municipal Health Bureau (20124323) and light of textile project (J201404). The authors would like to extend their sincere appreciation to the Deanship of Scientific Research at King Saud University for its funding of this research through the research group project no. RGP-201.

REFERENCES

1. R. A. Hoshi, R. Van Lith, M. C. Jen, J. B. Allen, K. A. Lapidos, and G. Ameer, The blood and vascular cell compatibility of heparin-modified ePTFE vascular grafts. *Biomaterials* 34, 30 (**2013**).
2. J. Wang, B. Zhou, X. Gu, M. Li, B. Gu, W. Wang, and Y. Li, Treatment of a canine carotid artery aneurysm model with a biodegradable nanofiber-covered stent: A prospective pilot study. *Neurology India* 61, 282 (**2013**).
3. A. Chandra, A. Suliman, and N. Angle, Spontaneous dissection of the carotid and vertebral arteries: The 10-year UCSD experience. *Annals of Vascular Surgery* 21, 178 (**2007**).
4. J. Wardlaw and P. White, The detection and management of unruptured intracranial aneurysms. *Brain* 123, 205 (**2000**).
5. I. Vulev and A. Klepanec, Aneurysm, edited by Y. Murai, Croatia InTech Publishers, Rijeka (**2012**), Vol. 1, pp. 249–268.
6. D. Angiletta, L. Maiellaro, D. Marinazzo, P. Wiesel, R. Pulli, and G. Regina, Endovascular management of type Ib endoleak complicating a juxtarenal aortic aneurysm previously treated with a multilayer stent. *Annals Of Vascular Surgery* 28, 5 (**2014**).
7. Y. D. Cho, H.-S. Kang, J. E. Kim, W.-S. Cho, H.-J. Kwon, H.-S. Koh, and M. H. Han, Modified protection using far proximal portion of self-expandable closed-cell stents for embolization of wide-necked intracranial aneurysms. *Neuroradiology* 56, 851 (**2014**).
8. X. H. He, W. T. Li, W. J. Peng, J. P. Lu, Q. Liu, and R. Zhao, Endovascular treatment of posttraumatic carotid-cavernous fistulas and pseudoaneurysms with covered stents. *Journal Of Neuroimaging* 24, 287 (**2014**).
9. S. K. Kim, J. Lee, J. R. Duncan, D. D. Picus, M. D. Darcy, and S. Sauk, Endovascular treatment of superior mesenteric artery pseudoaneurysms using covered stents in six patients. *AJR. American Journal of Roentgenology* 203, 432 (**2014**).
10. M.-H. Li, Y.-Q. Zhu, C. Fang, W. Wang, P.-L. Zhang, Y.-S. Cheng, H.-Q. Tan, and J.-B. Wang, The feasibility and efficacy of treatment with a Willis covered stent in recurrent intracranial aneurysms after coiling. *American Journal of Neuroradiology* 29, 1395 (**2008**).
11. M.-H. Li, Y.-D. Li, H.-Q. Tan, Q.-Y. Luo, and Y.-S. Cheng, Treatment of distal internal carotid artery aneurysm with the willis covered stent: A prospective pilot study1. *Radiology* 253, 470 (**2009**).
12. H.-Q. Tan, M.-H. Li, Y.-D. Li, C. Fang, J.-B. Wang, W. Wang, J. Wang, P.-L. Zhang, and Y.-Q. Zhu, Endovascular reconstruction with the Willis covered stent for the treatment of large or giant intracranial aneurysms. *Cerebrovascular Diseases* 31, 154 (**2010**).
13. S. Kawaguchi, T. Sakaki, H. Iwahashi, K. Fujimoto, J.-I. Iida, H. Mishima, and N. Nishikawa, Effect of carotid artery stenting on ocular circulation and chronic ocular ischemic syndrome. *Cerebrovascular Diseases* 22, 402 (**2006**).
14. J. H. Yang, H.-Y. Choi, H. S. Nam, S. H. Kim, S. W. Han, and J. H. Heo, Mechanism of infarction involving ipsilateral carotid and posterior cerebral artery territories. *Cerebrovascular Diseases* 24, 445 (**2007**).
15. P. Jamshidi, K. Mahmoody, and P. Erne, Covered stents: A review. *International Journal of Cardiology* 130, 310 (**2008**).
16. G. J. Laarman, F. Kiemeneij, R. Mueller, G. Guagliumi, M. Cobaugh, P. W. Serruys, and I. I. T. I. Symbiot, Feasibility, safety, and preliminary efficacy of a novel ePTFE-covered self-expanding stent in saphenous vein graft lesions: The Symbiot II trial. *Catheterization and Cardiovascular Interventions* 64, 361 (**2005**).
17. S. Yamaguchi, T. Asakura, S. Miura, T. Ohki, Y. Kanaoka, H. Ohta, N. Yajima, and M. Nakaya, Nonanastomotic rupture of thoracic aortic Dacron graft treated by endovascular stent graft placement. *General Thoracic and Cardiovascular Surgery* 61, 414 (**2013**).
18. H. S. Rangwala, C. N. Ionita, S. Rudin, and R. E. Baier, Partially polyurethane-covered stent for cerebral aneurysm treatment. *Journal Of Biomedical Materials Research Part B-Applied Biomaterials* 89B, 415 (**2009**).
19. J. J. Hu, W. C. Chao, P. Y. Lee, and C. H. Huang, Construction and characterization of an electrospun tubular scaffold for small-diameter tissue-engineered vascular grafts: A scaffold membrane approach. *J. Mech. Behav. Biomed. Mater.* 13, 140 (**2012**).

20. E. F. J. Chlupac and L. Bacakova, Blood vessel replacement: 50 years of development and tissue engineering paradigms in vascular surgery. *Physiol. Res.* 58, S119 (**2009**).

21. M. S. Lord, W. Yu, B. Cheng, A. Simmons, L. Poole-Warren, and J. M. Whitelock, The modulation of platelet and endothelial cell adhesion to vascular graft materials by perlecan. *Biomaterials* 30, 4898 (**2009**).

22. T. Chandy, G. S. Das, R. F. Wilson, and G. H. Rao, Use of plasma glow for surface-engineering biomolecules to enhance bloodcompatibility of Dacron and PTFE vascular prosthesis. *Biomaterials* 21, 699 (**2000**).

23. Z. Zhou and M. E. Meyerhoff, Preparation and characterization of polymeric coatings with combined nitric oxide release and immobilized active heparin. *Biomaterials* 26, 6506 (**2005**).

24. R. Hoover, R. Rosenberg, W. Haering, and M. Karnovsky, Inhibition of rat arterial smooth muscle cell proliferation by heparin. II. *In vitro* studies. *Circulation Research* 47, 578 (**1980**).

25. M. Princz and H. Sheardown, Heparin-modified dendrimer cross-linked collagen matrices for the delivery of basic fibroblast growth factor (FGF-2). *Journal of Biomaterials Science, Polymer Edition* 19, 1201 (**2008**).

26. O. Larm, R. Larsson, and P. Olsson, A new non-thrombogenic surface prepared by selective covalent binding of heparin via a modified reducing terminal residue. *Artificial Cells, Blood Substitutes and Biotechnology* 11, 161 (**1983**).

27. T. Asahara and J. M. Isner, Endothelial progenitor cells for vascular regeneration. *Journal of Hematotherapy and Stem Cell Research* 11, 171 (**2002**).

28. T. Asahara, T. Takahashi, H. Masuda, C. Kalka, D. Chen, H. Iwaguro, Y. Inai, M. Silver, and J. M. Isner, VEGF contributes to postnatal neovascularization by mobilizing bone marrow-derived endothelial progenitor cells. *The EMBO Journal* 18, 3964 (**1999**).

29. N. Ferrara, Vascular endothelial growth factor and the regulation of angiogenesis. *Recent Progress in Hormone Research* 55, 15; discussion 35-6 (**1999**).

30. R. D. Galiano, O. M. Tepper, C. R. Pelo, K. A. Bhatt, M. Callaghan, N. Bastidas, S. Bunting, H. G. Steinmetz, and G. C. Gurtner, Topical vascular endothelial growth factor accelerates diabetic wound healing through increased angiogenesis and by mobilizing and recruiting bone marrow-derived cells. *The American Journal of Pathology* 164, 1935 (**2004**).

31. E. Shantsila, T. Watson, and G. Y. Lip, Endothelial progenitor cells in cardiovascular disorders. *Journal of the American College of Cardiology* 49, 741 (**2007**).

32. C. Urbich and S. Dimmeler, Endothelial progenitor cells characterization and role in vascular biology. *Circulation Research* 95, 343 (**2004**).

33. A. H. Dorafshar, N. Angle, M. Bryer-Ash, D. Huang, M. M. Farooq, H. A. Gelabert, and J. A. Freischlag, Vascular endothelial growth factor inhibits mitogen-induced vascular smooth muscle cell proliferation. *Journal of Surgical Research* 114, 179 (**2003**).

34. H. Zhang, X. Jia, F. Han, J. Zhao, Y. Zhao, Y. Fan, and X. Yuan, Dual-delivery of VEGF and PDGF by double-layered electrospun membranes for blood vessel regeneration. *Biomaterials* 34, 2202 (**2013**).

35. F. Du, H. Wang, W. Zhao, D. Li, D. Kong, J. Yang, and Y. Zhang, Gradient nanofibrous chitosan/poly varepsilon-caprolactone scaffolds as extracellular microenvironments for vascular tissue engineering. *Biomaterials* 33, 762 (**2012**).

36. G. Denas and V. Pengo, Current anticoagulant safety. *Expert Opinion on Drug Safety* 11, 401 (**2012**).

37. A. Gomez-Outes, M. L. Suarez-Gea, R. Lecumberri, E. Rocha, C. Pozo-Hernandez, and E. Vargas-Castrillon, New parenteral anticoagulants in development. *Therapeutic Advances in Cardiovascular Disease* 5, 33 (**2011**).

38. P. B. Salbach, M. Bruckmann, O. Turovets, J. Kreuzer, W. Kubler, and I. Walter-Sack, Heparin-mediated selective release of hepatocyte growth factor in humans. *British Journal Of Clinical Pharmacology* 50, 221 (**2000**).

39. G. Ranieri, R. Patruno, E. Ruggieri, S. Montemurro, P. Valerio, and D. Ribatti, Vascular endothelial growth factor (VEGF) as a target of bevacizumab in cancer: From the biology to the clinic. *Current Medicinal Chemistry* 13, 1845 (**2006**).

40. N. Ferrara, Role of vascular endothelial growth factor in Physiologic and Pathologic angiogenesis: Therapeutic implications. *Seminars In Oncology* 29, 10 (**2002**).

41. R. K. Jain, Tumor angiogenesis and accessibility: Role of vascular endothelial growth factor. *Seminars In Oncology* 29, 3 (**2002**).

42. S. Takeshita, L. Zheng, E. Brogi, M. Kearney, L. Pu, S. Bunting, N. Ferrara, J. Symes, and J. Isner, Therapeutic angiogenesis. A single intraarterial bolus of vascular endothelial growth factor augments revascularization in a rabbit ischemic hind limb model. *Journal of Clinical Investigation* 93, 662 (**1994**).

43. Y. Yang, X. Li, S. He, L. Cheng, F. Chen, S. Zhou, and J. Weng, Biodegradable ultrafine fibers with core-sheath structures for protein delivery and its optimization. *Polymers for Advanced Technologies* 22, 1842 (**2011**).

44. X. Xu, X. Chen, P. Ma, X. Wang, and X. Jing, The release behavior of doxorubicin hydrochloride from medicated fibers prepared by emulsion-electrospinning. *Eur. J. Pharm Biopharm.* 70, 165 (**2008**).

45. W. Ji, Y. Sun, F. Yang, J. J. van den Beucken, M. Fan, Z. Chen, and J. A. Jansen, Bioactive electrospun scaffolds delivering growth factors and genes for tissue engineering applications. *Pharm Res.* 28, 1259 (**2011**).

46. Y. Yang, X. Li, M. Qi, S. Zhou, and J. Weng, Release pattern and structural integrity of lysozyme encapsulated in core-sheath structured poly(DL-lactide) ultrafine fibers prepared by emulsion electrospinning. *Eur. J. Pharm Biopharm.* 69, 106 (**2008**).

47. X. Zhao and M. Hadjiargyrou, Induction of cell migration *in vitro* by an electrospun PDGF-BB/PLGA/PEG-PLA nanofibrous scaffold. *Journal of Biomedical Nanotechnology* 7, 823 (**2011**).

48. K. T. Shalumon, S. Sowmya, D. Sathish, K. P. Chennazhi, S. V. Nair, and R. Jayakumar, Effect of incorporation of nanoscale bioactive glass and hydroxyapatite in PCL/chitosan nanofibers for bone and periodontal tissue engineering. *Journal of Biomedical Nanotechnology* 9, 430 (**2013**).

49. M. Jaiswal, A. Gupta, A. K. Agrawal, M. Jassal, A. K. Dinda, and V. Koul, Bi-Layer composite dressing of gelatin nanofibrous mat and poly vinyl alcohol hydrogel for drug delivery and wound healing application: *In-vitro* and *in-vivo* studies. *Journal Of Biomedical Nanotechnology* 9, 1495 (**2013**).

50. Q. Wang, N. Zhang, X. W. Hu, J. H. Yang, and Y. M. Du, Alginate/polyethylene glycol blend fibers and their properties for drug controlled release. *Journal Of Biomedical Materials Research Part A* 82A, 122 (**2007**).

51. L. M. Jiang, H. Z. Sun, A. L. Yuan, K. Zhang, D. W. Li, C. Li, C. Shi, X. W. Li, K. Gao, C. Y. Zheng, B. Yang, and H. C. Sun, Enhancement of osteoinduction by continual simvastatin release from poly(lactic-co-glycolic acid)-hydroxyapatite-simvastatin nanofibrous scaffold. *Journal of Biomedical Nanotechnology* 9, 1921 (**2013**).

52. T. H. B. Eriksen, E. Skovsen, and P. Fojan, Release of antimicrobial peptides from electrospun nanofibres as a drug delivery system. *Journal Of Biomedical Nanotechnology* 9, 492 (**2013**).

53. Y. Dai, J. Niu, J. Liu, L. Yin, and J. Xu, *In situ* encapsulation of laccase in microfibers by emulsion electrospinning: Preparation, characterization, and application. *Bioresour. Technol.* 101, 8942 (**2010**).

54. X. Li, Y. Su, S. Liu, L. Tan, X. Mo, and S. Ramakrishna, Encapsulation of proteins in poly(L-lactide-co-caprolactone) fibers by emulsion electrospinning. *Colloids Surf B Biointerfaces* 75, 418 (**2010**).

55. X. Luo, C. Xie, H. Wang, C. Liu, S. Yan, and X. Li, Antitumor activities of emulsion electrospun fibers with core loading of hydroxycamptothecin via intratumoral implantation. *Int. J. Pharm.* 425, 19 (**2012**).

56. L. Tian, M. P. Prabhakaran, X. Ding, D. Kai, and S. Ramakrishna, Emulsion electrospun vascular endothelial growth factor encapsulated poly(l-lactic acid-co-ε-caprolactone) nanofibers for sustained release in cardiac tissue engineering. *Journal of Materials Science* 47, 3272 **(2011)**.

57. A. L. Yarin, Coaxial electrospinning and emulsion electrospinning of core–shell fibers. *Polymers for Advanced Technologies* 22, 310 **(2011)**.

58. K. T. Shalumon, K. P. Chennazhi, S. V. Nair, and R. Jayakumar, Development of small diameter fibrous vascular grafts with outer wall multiscale architecture to improve cell penetration. *Journal Of Biomedical Nanotechnology* 9, 1299 **(2013)**.

59. L. Jin, T. Wang, M.-L. Zhu, M. K. Leach, Y. I. Naim, J. M. Corey, Z.-Q. Feng, and Q. Jiang, Electrospun fibers and tissue engineering. *Journal of Biomedical Nanotechnology* 8, 1 **(2012)**.

60. P. R. Sreerekha, D. Menon, S. V. Nair, and K. P. Chennazhi, Fabrication of fibrin based electrospun multiscale composite scaffold for tissue engineering applications. *Journal Of Biomedical Nanotechnology* 9, 790 **(2013)**.

61. S. J. Xin, X. Y. Li, Q. Wang, R. Huang, X. L. Xu, Z. J. Lei, and H. B. Deng, Novel layer-by-layer structured nanofibrous mats coated by protein films for dermal regeneration. *Journal Of Biomedical Nanotechnology* 10, 803 **(2014)**.

62. J. B. Lee, H. N. Park, W. K. Ko, M. S. Bae, D. N. Heo, D. H. Yang, and I. K. Kwon, Poly(L-lactic acid)/Hydroxyapatite nanocylinders as nanofibrous structure for bone tissue engineering scaffolds. *Journal Of Biomedical Nanotechnology* 9, 424 **(2013)**.

63. I. H. L. Pereira, E. Ayres, L. Averous, G. Schlatter, A. Hebraud, A. C. C. de Paula, P. H. L. Viana, A. M. Goes, and R. L. Orefice, Differentiation of human adipose-derived stem cells seeded on mineralized electrospun co-axial poly(epsilon-caprolactone) (PCL)/gelatin nanofibers. *Journal Of Materials Science-Materials In Medicine* 25, 1137 **(2014)**.

64. K. E. Park, H. K. Kang, S. J. Lee, B. M. Min, and W. H. Park, Biomimetic nanofibrous scaffolds: Preparation and characterization of PGA/chitin blend nanofibers. *Biomacromolecules* 7, 635 **(2006)**.

65. J. P. Chen, G. Y. Chang, and J. K. Chen, Electrospun collagen/chitosan nanofibrous membrane as wound dressing. *Colloids And Surfaces A-Physicochemical and Engineering Aspects* 313, 183 **(2008)**.

66. F. Y. Ding, H. B. Deng, Y. M. Du, X. W. Shi, and Q. Wang, Emerging chitin and chitosan nanofibrous materials for biomedical applications. *Nanoscale* 6, 9477 **(2014)**.

67. C. Wu, Q. An, D. Li, J. Wang, L. He, C. Huang, Y. Li, W. Zhu, and X. Mo, A novel heparin loaded poly(l-lactide-co-caprolactone) covered stent for aneurysm therapy. *Materials Letters* 116, 39 **(2014)**.

68. Z.-M. Huang, Y. Zhang, S. Ramakrishna, and C. Lim, Electrospinning and mechanical characterization of gelatin nanofibers. *Polymer* 45, 5361 **(2004)**.

69. S. Yan, L. Xiaoqiang, T. Lianjiang, H. Chen, and M. Xiumei, Poly(l-lactide-co-ε-caprolactone) electrospun nanofibers for encapsulating and sustained releasing proteins. *Polymer* 50, 4212 **(2009)**.

70. K. Wang, Q. Huang, B. Hong, Y. Xu, W. Zhao, J. Chen, R. Zhao, and J. Liu, Neck injury is critical to elastase-induced aneurysm model. *American Journal of Neuroradiology* 30, 1685 **(2009)**.

71. R. B. M. J. B. Wissink, J. S. Pieper, A. A. Poot, G. H. M. Engbers, T. Beugelin, W. G. van Aken, and J. Feijen*, Immobilization of heparin to EDC/NHS-crosslinked collagen characterization and *in vitro* evaluation. *Biomaterials* 22, 151 **(2001)**.

72. L. Liu, S. Guo, J. Chang, C. Ning, C. Dong, and D. Yan, Surface modification of polycaprolactone membrane via layer-by-layer deposition for promoting blood compatibility. *J. Biomed. Mater. Res. B Appl. Biomater.* 87, 244 **(2008)**.

73. P. Y. Tseng, S. S. Rele, X. L. Sun, and E. L. Chaikof, Membrane-mimetic films containing thrombomodulin and heparin inhibit tissue factor-induced thrombin generation in a flow model. *Biomaterials* 27, 2637 **(2006)**.

74. X. Jia, C. Zhao, P. Li, H. Zhang, Y. Huang, H. Li, J. Fan, W. Feng, X. Yuan, and Y. Fan, Sustained release of VEGF by coaxial electrospun dextran/PLGA fibrous membranes in vascular tissue engineering. *Journal of Biomaterials Science, Polymer Edition* 22, 1811 **(2011)**.

75. S. I. Jeong, B. S. Kim, S. W. Kang, J. H. Kwon, Y. M. Lee, S. H. Kim, and Y. H. Kim, *In vivo* biocompatibilty and degradation behavior of elastic poly(L-lactide-co-epsilon-caprolactone) scaffolds. *Biomaterials* 25, 5939 **(2004)**.

76. X. M. Mo, C. Y. Xu, M. Kotaki, and S. Ramakrishna, Electrospun P(LLA-CL) nanofiber: A biomimetic extracellular matrix for smooth muscle cell and endothelial cell proliferation. *Biomaterials* 25, 1883 **(2004)**.

77. X. Li, Y. Su, X. Zhou, and X. Mo, Distribution of Sorbitan Monooleate in poly(l-lactide-co-ε-caprolactone) nanofibers from emulsion electrospinning. *Colloids and Surfaces B: Biointerfaces* 69, 221 **(2009)**.

78. L. Wu, H. Li, S. Li, X. Li, X. Yuan, X. Li, and Y. Zhang, Composite fibrous membranes of PLGA and chitosan prepared by coelectrospinning and coaxial electrospinning. *J. Biomed. Mater. Res. A* 92, 563 **(2010)**.

79. D. B. Pike, S. S. Cai, K. R. Pomraning, M. A. Firpo, R. J. Fisher, X. Z. Shu, G. D. Prestwich, and R. A. Peattie, Heparin-regulated release of growth factors *in vitro* and angiogenic response *in vivo* to implanted hyaluronan hydrogels containing VEGF and bFGF. *Biomaterials* 27, 5242 **(2006)**.

80. X. W. Y. Z. Zhang, Y. Feng, J. Li, C. T. Lim, and S. Ramakrishna, Coaxial electrospinning of (fluorescein isothiocyanate-conjugated bovine serum albumin)-encapsulated poly(e-caprolactone) nanofibers for sustained release. *Biomacromolecules* 7, 1049 **(2006)**.

81. K. Zhang, A. Yin, C. Huang, C. Wang, X. Mo, S. S. Al-Deyab, and M. El-Newehy, Degradation of electrospun SF/P(LLA-CL) blended nanofibrous scaffolds *in vitro*. *Polymer Degradation and Stability* 96, 2266 **(2011)**.

82. J. Wu, C. Huang, W. Liu, A. Yin, W. Chen, C. He, H. Wang, S. Liu, C. Fan, G. L. Bowlin, and X. Mo, Cell infiltration and vascularization in porous nanoyarn scaffolds prepared by dynamic liquid electrospinning. *Journal of Biomedical Nanotechnology* 10, 603 **(2014)**.

83. M. I. Santos, K. Tuzlakoglu, S. Fuchs, M. E. Gomes, K. Peters, R. E. Unger, E. Piskin, R. L. Reis, and C. J. Kirkpatrick, Endothelial cell colonization and angiogenic potential of combined nano- and microfibrous scaffolds for bone tissue engineering. *Biomaterials* 29, 4306 **(2008)**.